Scalable Computing: Practice and Experience, ISSN 1895-1767, http://www.scpe.org
© 2024 SCPE. Volume 25, Issues 2, pp. 1124–1133, DOI 10.12694/scpe.v25i2.2654

INTELLIGENT NAVIGATION SYSTEM BASED ON BIG DATA TRAFFIC SYSTEM

XIU ZHANG*, JIAN KANG†, AND HAICUN YU‡

Abstract. This paper studies the navigation technology of the On-Orbit Servicing Spacecraft (OSS) and proposes an overall solution for the OSS navigation system. The composition of the OSS satellite navigation simulation system and simulation supporting environment are studied. Then a new SSUKF navigation filter is proposed based on the hyper spherical distributed feature sampling point transform algorithm (SSUT) and the non-scanning Kalman filter (UKF). The numerical simulation of the OSS system is studied based on MATLAB/RTW. Finally, the SSUKF algorithm and the conventional UKF algorithm are simulated digitally. The effectiveness and advanced nature of the hybrid Kalman filter applied to spacecraft autonomous navigation are verified.

Key words: Spacecraft; Big data; Hyperspherical distributed sampling point transformation algorithm; Unscented Kalman filtering; Navigation system

1. Introduction. A spacecraft's autonomous navigation system uses its own load or observation instrument to realize the precise positioning of the spacecraft and motion trajectory. Since 1963, the United States has carried out in-depth research on the autonomous navigation of satellites and developed various types of sensitive elements and space navigation systems. In recent years, significant progress has been made in studying small satellites and microsatellites in China. At present, autonomous navigation has gradually become one of the leading indicators to measure the comprehensive capability of spacecraft. It is found that the GNC system has the highest failure probability based on the statistics of spacecraft failure probability data in the recent ten years. A navigation system is an essential part of the GNC system. The "rendezvous" and "docking" part of the open satellite is the crucial part of the whole flight satellite navigation system [1]. The approach segment of the image guidance scheme employed by OE uses infrared cameras (IRS) to back up advanced image guidance sensors (AVGS). But the IRS's adequate scope does not cover all approximate segments. When AVGS fails during the approach process, replacing the spare sensitive element is unnecessary to perform the on-orbit mission. The vehicle uses RGPS navigation. Communication between spacecraft is essential. Due to the large number of non-cooperative targets in space, coupled with the existing domestic relay communication system has not reached, the world can only use RGPS technology.

Unsampled Kalman filter (UKF) is a state estimation method based on unsampled transformation. The nonlinear control method based on UKF is superior to the traditional Kalman filter and has a broad application prospect. The calculation speed of the UKF method mainly depends on the number of sample points in the unscanned transformation. The conventional UKF algorithm performs unsampled conversion on 2n+1 sampling points. The sampling point is symmetric concerning the mean of the n-dimensional vector. Because the vector dimension is too large, the operation speed of the algorithm will be reduced [2]. This project will adopt Superball Distribution Transform (SSUT) to replace the traditional symmetric distribution. The algorithm can effectively reduce the number of samples and improve the algorithm's efficiency without affecting the filtering effect. The thesis uses MATLAB/RTW as the platform to study the positioning of OSS. A new SSUKF navigation filter is proposed by fusing SSUT and UKF. The algorithm is applied to the autonomous navigation algorithm of spacecraft using starlight Angle distance as observation information.

2. The overall scheme of the OSS navigation simulation system.

*Department of Information Technology, Tangshan Vocational and Technical College, Tangshan, 063000, China
†Department of Information Technology, Tangshan Vocational and Technical College, Tangshan, 063000, China
‡Department of Information Technology, Tangshan Vocational and Technical College, Tangshan, 063000, China (Corresponding author, tsvtczhangxiu@126.com)

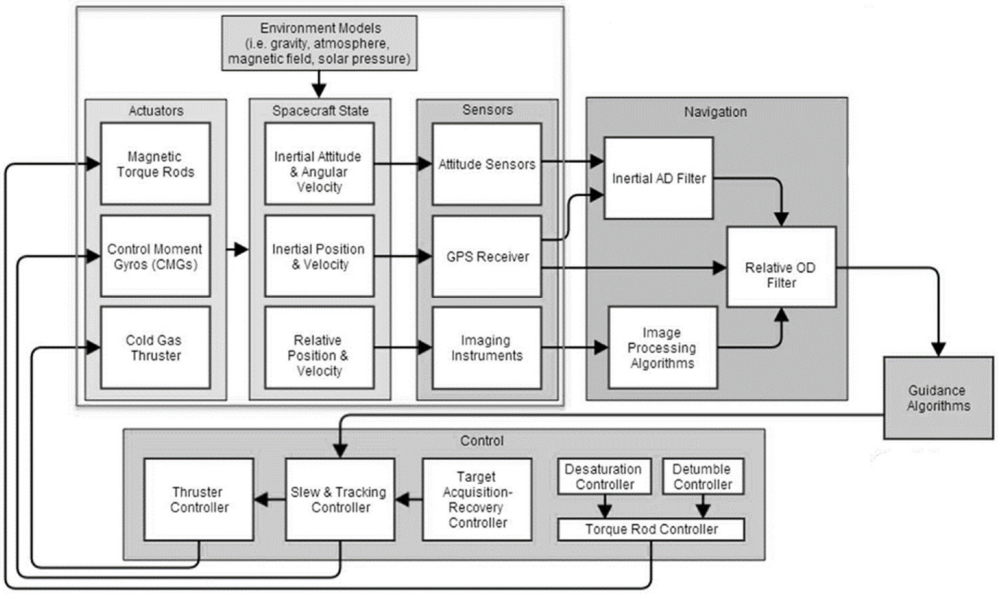

Fig. 2.1: Overall simulation architecture of OSS navigation system.

OSS Navigation System Mission Planning	Simulation support environment based on MATLAB/RTW
Tracking Spacecraft Orbit Mission Planning	Simulation run process control
Target spacecraft orbit mission planning	Simulation running status monitoring
Spacecraft on-orbit mission planning	Simulation Data Management
Spacecraft Rendezvous Mission Planning	Communication settings and management between data
Tracking Spacecraft Propulsion Strategy Planning	Simulation Data Visualization
Strategy planning for autonomous operation of navigation system in orbit	
OSS Navigation System Simulation	OSS Navigation System Performance Evaluation
OSS Orbital Dynamics	System Integrity Performance Assessment
Target spacecraft orbital dynamics	GNSS Constellation Performance Evaluation
Satellite Navigation Simulation	Performance Evaluation of Spaceborne GNSS Receiver
Inertial Navigation Simulation	Performance Evaluation of Spaceborne Inertial Measurement Units
Celestial Navigation Simulation	Performance Evaluation of Spaceborne Celestial Navigation Measurement Components
Data Processing and Information Fusion	Performance Evaluation of Spaceborne Relative Navigation Measurement Components
Relative Navigation Simulation	Performance Evaluation of Spaceborne Image Navigation Measurement Components
Image Navigation Simulation	Performance Evaluation of Spaceborne GNSS Navigation
Space Environment Effects and Observational Data Generation	Performance Evaluation of Spaceborne Inertial Navigation
Navigation data runs autonomously	Performance Evaluation of Spaceborne Celestial Navigation
	Performance Evaluation of Spaceborne Relative Navigation
	Performance Evaluation of Spaceborne Image Navigation
	Navigation Mode and Integrated Navigation Performance Evaluation

Fig. 2.2: Functional structure.

2.1. Simulation system architecture. Using MATLAB/RTW as the platform, the simulation of the OSS in-orbit mission, navigation system requirements, navigation sensor setup and navigation mode is carried out. Its overall simulation architecture is shown in Figure 2.1. The functional structure of the OSS navigation simulation system is shown in Figure 2.2. The simulation system mainly includes the following four parts:

2.1.1. OSS Navigation System Task Planning. A scheme for tracking the flight path between the spacecraft and the target spacecraft is proposed. The planning problems of spacecraft in orbit and rendezvous flight are studied [3]. It lays a foundation for tracking the propulsion and autonomous operation of the satellite in orbit and its motion trajectory. The satellite's flight path will also provide a necessary reference for the regular operation and test of the simulator.

2.1.2. Simulation of OSS navigation system. The OSS navigation system is simulated according to the flight plan. The comprehensive performance of the system under various navigation modes, error influencing factors and coordination of subsystems are studied [4]. The OSS navigation system consists of 10 sub-modules: OSS orbit dynamics, target spacecraft orbit Dynamics, satellite navigation, inertial navigation, astronomical navigation, data processing and information fusion, relative navigation, image navigation, space environment impact and observation data generation, and navigation data autonomous operation.

2.1.3. Support simulation system implemented by MATLAB/RTW. The supporting environment provides an operational platform for the system's planning, simulation and evaluation. According to the requirement of a real-time system, the system is divided into two categories: real-time class and non-real-time class [5]. The supporting environment can configure the system in real-time for various real-time requirements. Some basic algorithms, noise simulation and data processing are provided.

2.1.4. Performance evaluation of OSS navigation system. The performance of the system is evaluated based on numerical simulation. The performance evaluation of OSS based navigation sensor and navigation system is completed. Various fault and error factors are analyzed [6]. It lays a theoretical foundation for the research of semi-physical and physical simulation.

2.2. Key system technologies.

2.2.1. Synchronizing Data with Time Series. Each sensor has its own time. Taking GNSS as an example, the target's pose is obtained by the observed pseudo-distance/pseudo-distance rate combined with the star vector observed by STR. Their calculations are based on their clocks. This paper designs a unique clock for the simulation system. Each subsystem has orders. Turn functionality into your clock. It is necessary to divide the timing of each module reasonably to ensure that the simulation performance of each sensor and filter element in the OSS system simulation meets specific causes and consequences. The causal relationship between data transmission synchronization and data transmission needs to be clarified. Synchronous transmission is after OSS generates new trajectory information [7]. The OSS generates new trajectory information, and the receiver generates new trajectory information—the message flow limits data transmission synchronization. It is necessary to use the orbit data of OSS. This paper presents a guidance algorithm based on fuzzy logic to ensure the correctness of the information transmission.

2.2.2. Fault Detection, Isolation, and Repair (FDIR). Open-source analysis software is a kind of nonlinear system with dynamic properties. The operation of sensors and actuators must be monitored in real-time during simulated flight. FDIR guarantees the autonomy of an open service system. The system can monitor and analyze the operation of open-source systems [8]. Evaluate the current sensor performance and feedback OSS performance to MVM. An intelligent positioning technology based on OSS is proposed and verified by experiments. An intelligent diagnosis method based on fuzzy logic is proposed. The model uses database technology to express the required knowledge in a particular form. Thus, a knowledge base of expert systems is formed [9]. An expert system based on logical reasoning is constructed using a particular programming language. The knowledge database is maintained and updated.

2.2.3. Guide mode conversion method. The primary purpose of navigation mode switching is to ensure the precise and safe switching of OSS in orbit. The navigation system model is managed based on events, moments, and observations from navigation sensors in the OSS flight plan [10]. Determine the current health of open-source software. Triggers the corresponding guidance sensor to start and transmit pattern initialization parameters. Use related data as separate states to express different browsing patterns. Events are set as status start and transfer operations. Develop processes for state transitions in event-driven situations [11]. Transform between navigation modes with State flow and embed it in Simulink. Convert it into an executable program via RTW and download it to the destination system.

3. SSUKF navigation filtering algorithm.

3.1. Superball distribution sampling conversion UKF. The navigation filtering system of generalized Kalman filtering technology is widely used. However, the generalized Kalman filter has problems, such as difficult debugging, unstable performance when it does not meet the linearization conditions, and the need to

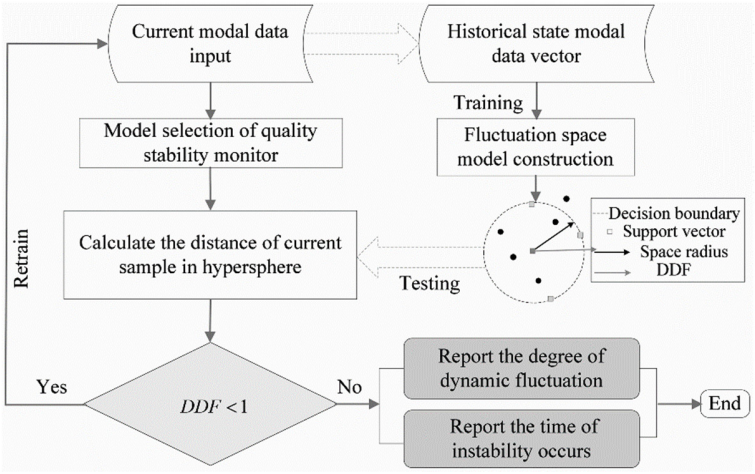

Fig. 3.1: Flow of hyper spherical distributed sampling transformation algorithm.

calculate the Jacobian matrix. The University of Oxford introduced the Superball Point Force Family (UKF) method in this field in the 1990s to overcome the above defects. UKF uses a set of recursive equations similar to Kalman filters. The prior knowledge is used to iterate the system state and system parameters. Then the system parameters are modified according to the relevant knowledge of the observation time point to achieve the average of the system state and parameter estimation. UKF differs from an extended Kalman filter in using a set of sample points. These sample points are close to the Gaussian distribution [12]. The method uses a non-minimization transformation to recurse and modify the covariance of the system state and deviation, thus avoiding the solution of the Jacobian matrix of the system state and the observation system. It is also relatively easy to implement. The basic idea of the EKF algorithm is to carry out Taylor expansion of the system at the measured point without considering the higher order terms of the second order or more [13]. The UKF algorithm approximates the state of the system through non-segmentation transformation. Compared with the EKF algorithm, this algorithm can achieve quadratic or even higher accuracy. Therefore, the accuracy of this algorithm is higher than that of the EKF algorithm. In addition, UKF also adds unconstrained transformation in iteration so that the adjustment coefficient required in an iteration is more than EKF. Its debugging is more flexible. The UKF method is similar to the EKF method in that both are estimates of serialized state parameters [14]. The recursive steps of the structure flow are also composed of the propagation of state and covariance and the updating of measurements. Figure 3.1 shows the Flow of the hyper spherical distributed sampling transformation algorithm (The picture is quoted in the Journal of Process Mechanical Engineering. 2019; 233(3):436-447).

3.2. SSUT. Suppose x is a n dimensional random variable. The mean matrix is $\hat{x}$ and the mean square error matrix is Q_{xx}. x random variable y of $y = g(x)$ dimension is obtained after a nonlinear transformation $y = g(x)$ is performed on a. The non-sampling conversion method is to select x set of samples that can represent the mean and variance of sample x. By using this method, a nonlinear transformation of y is carried out, and the converted sample is used to approximate y.

For non-scan conversion, $2n + 1$ sample points with uniform distribution are generally selected [15]. It is generally required to have more than $n+1$ samples to describe the mean and variance number of n-dimensional state variables. The probability distribution of the system is approximated by taking $n + 1$ samples with the same weight on the hypersphere. This sample point is combined with the mean of its states to form a $n + 2$ sample point without sampling transformation. The mean square error matrix of n dimension z is an identity matrix, and the sampling method on the hypersphere is as follows:

1) Option valueω_0.

$$0 \le \omega_0 \le 1 \tag{3.1}$$

2) Determine weight ω_i:

$$\begin{aligned} &\omega_i = (1-\omega_0)/(n+1) \\ &i = 1, \ldots, n+1 \end{aligned} \tag{3.2}$$

3) Initialize vector sequence:

$$\left.\begin{aligned} &R_0^1 = [0] \\ &R_1^1 = [-1/\sqrt{2\omega_1}] \\ &R_2^1 = [1/\sqrt{2\omega_1}] \end{aligned}\right\} \tag{3.3}$$

4) Extension vector sequence ($j = 2, \cdots, n$):

$$R_i^j = \begin{cases} \begin{bmatrix} R_0^{j-1} \\ 0 \end{bmatrix} & i = 0 \\ \begin{bmatrix} R_i^{j-1} \\ -1/\sqrt{j(j+1)\omega_j} \end{bmatrix} & i = 1, \ldots, j \\ \begin{bmatrix} 0^{j-1} \\ j/\sqrt{j(j+1)\omega_j} \end{bmatrix} & i = j+1 \end{cases} \tag{3.4}$$

R_i^j represents the i sampling point of a $j$dimensional random variable. 0^j stands for $j$dimensional zero vector. $n+2$ sampling points $R_i^n, i = 0, \ldots, n+1$ of z are obtained by the above method [16]. The number of super-spherical distribution samples for a $n$dimensional random variable $x$with mean value of $\hat{x}$ and mean square error matrix of Q_{xx} can be obtained from formula (3.5):

$$X_i^n = \hat{x} + \sqrt{Q_{xx}} R_i^n \quad i = 0, \ldots, n+1 \tag{3.5}$$

3.3. UKF algorithm based on SSUT. Suppose that the equations of state and measurement for a nonlinear system are expressed in the following discrete form:

$$x_{t+1} = G(x_t, A_t, t) + \delta_t \tag{3.6}$$

$$y_t = H(x_t, t) + \varepsilon_t \tag{3.7}$$

x_t is the system state vector. A_t is the input control vector. y_t is the observation vector. δ_t and ε_t are the system noise vector and the measurement noise vector respectively. The mean is 0. The variance matrix is denoted by Q_t and S_t, respectively. Let the system state vector dimension be$n$.

3.4. Mathematical model of the autonomous navigation system.

3.4.1. Spacecraft orbital motion model. The geocentric equatorial inertial coordinate system establishes the spacecraft orbital motion equation. A two-body motion model with harmonic terms, including the second-order perturbation of the earth's gravitational field, is taken [17]. The other perturbation factors are

equivalent to Gaussian white noise.

$$\left.\begin{aligned}
\frac{dx}{dt} &= \varepsilon_x \\
\frac{dy}{dt} &= \varepsilon_y \\
\frac{dz}{dt} &= \varepsilon_z \\
\frac{d\varepsilon_x}{dt} &= -\lambda\frac{x}{s^3}\left[1 - H_2\left(\frac{S_R}{s}\right)^2 \cdot \left(7.5\frac{z^2}{s^2} - 1.5\right)\right] + \delta_{\varepsilon_x} \\
\frac{d\varepsilon_y}{dt} &= -\lambda\frac{y}{s^3}\left[1 - H_2\left(\frac{S_R}{s}\right)^2 \cdot \left(7.5\frac{z^2}{s^2} - 1.5\right)\right] + \delta_{\varepsilon_y} \\
\frac{d\varepsilon_z}{dt} &= -\lambda\frac{z}{s^3}\left[1 - H_2\left(\frac{S_R}{s}\right)^2 \cdot \left(7.5\frac{z^2}{s^2} - 4.5\right)\right] + \delta_{\varepsilon_z}
\end{aligned}\right\} \tag{3.8}$$

$s = \sqrt{x^2 + y^2 + z^2}; x, y, z$ is the position coordinate of the spacecraft. $\varepsilon_x, \varepsilon_y, \varepsilon_z$ is the velocity coordinate of the spacecraft. λ is the gravitational constant of the earth. H_2 is the second order harmonic term coefficient of the earth. S_R is the earth's equatorial radius. $\delta_{\varepsilon_x}, \delta_{\varepsilon_y}, \delta_{\varepsilon_z}$ is system noise.

3.4.2. Starlight angular distance measurement model. The angular distance of starlight can be determined according to the measurement information of the infrared earth sensor and star sensor. The angle between the vector direction of the light of the navigation star and the vector direction of the earth's center in the spacecraft body coordinate system. Starlight angular distance remains constant in different coordinate systems. The angular distance measured in the body coordinate system can also be used in the equatorial inertial coordinate system [18]. In the geocentric equatorial inertial coordinate system, the expression of starlight angular distance between the two navigation stars is

$$\theta_1 = \beta_1 + \varepsilon_{\theta_1} = \arccos\left(-\frac{xB_{x_1} + yB_{y_1} + zB_{z_1}}{s}\right) + \varepsilon_{\theta_1} \tag{3.9}$$

$$\theta_2 = \beta_2 + \varepsilon_{\theta_2} = \arccos\left(-\frac{xB_{x_2} + yB_{y_2} + zB_{z_2}}{s}\right) + \varepsilon_{\theta_2} \tag{3.10}$$

$B_{x_1}, B_{y_1}, B_{z_1}$ and $B_{x_2}, B_{y_2}, B_{z_2}$ are the direction cosine of the two navigation stars in the geocentric equatorial inertial coordinate system, respectively.

4. SSUKF-EKF hybrid filter design. The UKF method does not need to linearize the observation equation and the equation of state when solving nonlinear problems. The method has no truncation error of higher-order terms. The algorithm has fast convergence and high steady-state accuracy. At the same time, the method has strong robustness to random disturbance. UKF algorithm needs to process multiple sampling points simultaneously in a period, which leads to slow algorithm convergence. EKF algorithm is an efficient algorithm. At the same time, the method has higher accuracy in the case of weakening the nonlinearity [19]. However, the EKF will diverge when there are large initial values and random noise. Since the operation steps of the two methods are based on the Kalman filter, the two methods can be combined to construct the Kalman filter. The Flow of the SSUKF-EKF hybrid filter algorithm is illustrated in Figure 4.1 (image quoted in Journal of neural engineering.13.10.1109 / ICVR.2015.7358598.) M is a function that increases as the accuracy of the parameter estimation increases. This paper presents the EKF method. If the value of a function exceeds an error threshold, it indicates that the filtering effect of the function becomes worse to improve the computing speed. An improved SSUKF method is proposed. Kalman filter has strong robustness in practical applications, and its stability depends on the state of the system and the measurement equation. Its stability is good if the Kalman filter has random controllability and random observability. The method uses the modal conversion

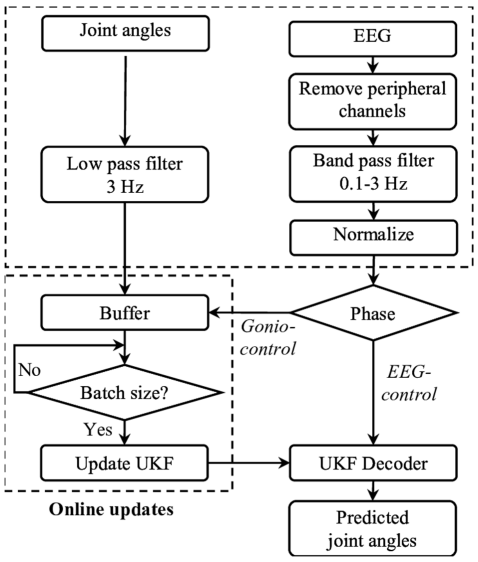

Fig. 4.1: Hybrid Kalman filter algorithm flow.

function and error threshold of EKF and UKF to realize the adaptive conversion of the two algorithms. This is only a few changes to the mean and variance matrix operation and does not affect its stability [20]. Therefore, selecting the proper minimum root mean square can improve the filtering effect while ensuring accuracy.

5. System implementation and numerical simulation.

5.1. System Implementation. This paper studies the OSS navigation simulation system based on MATLAB/RTW. RTW is an auxiliary graphical model and simulation system. The software converts the Simulink model into an improved, portable, personalized program [21]. Different application scenarios can be generated automatically based on different object structures. Real-time hyper spherical communication technology communicates with multiple targets. RTW provides an accelerated simulation method for processing batch simulations, such as the Monte Carlo shooting type. In addition, the external mode Simulink of RTW can communicate with the model system in the real-time simulation environment to achieve real-time simulation control, operating state monitoring, parameter adjustment and data observation. The architecture block diagram for rapid prototyping of the OSS navigation system using MATLAB/RTW is shown in Figure 5.1 (Electronics 2022,113,1979).

This paper uses MATLAB and Simulink toolkits to study the navigation simulator's overall scheme. The models of each subsystem are established. The flow chart of the system is drawn, and numerical simulation is carried out. The Monte Carlo statistical method is used to evaluate and analyze the performance [22]. The proposed method is improved and applied to the navigation system. The application of Simulink in practical applications is realized using RTW technology—real-time functional verification in external mode.

5.2. Numerical Simulation. The equatorial inertial system at the center of the H2000 Earth is used as coordinates. The parameters of the initial orbit are as follows: Long semi-axis a=7151.918 km—eccentricity e=0.5. The earth's tilt is 98.52°. The correct longitude of the ascending node is 234.083°. The perigee oscillation Angle is 234.083°. Horizontal approach points 240.817°. Sensitivity accuracy includes 1 "star-containing and 0.01-degree infrared Earth sensitivity accuracy. The measurement noise is treated as a normal distribution. The aspherical gravity perturbations of the earth are calculated in the actual operation [23]. In this paper, the earth gravity model is established by using JGM3. The fourth-order Rungkat method is proposed. The numerical simulation of the problem is carried out in the case of solar and lunar gravity, atmospheric drag, solar light pressure and other disturbances.

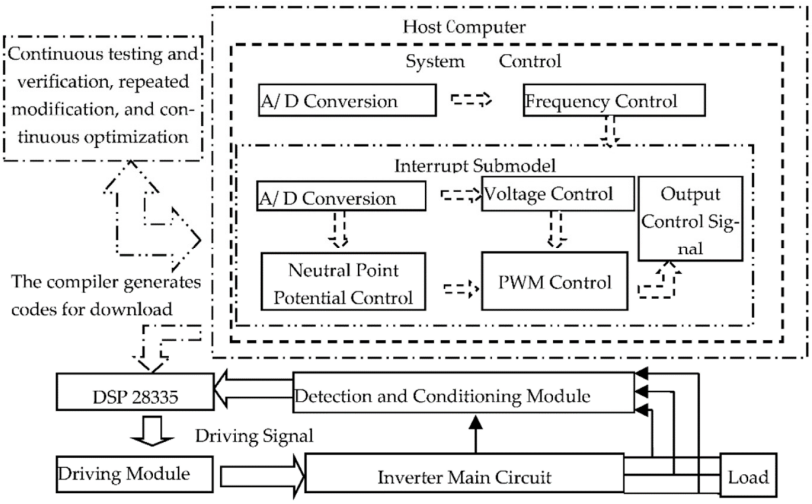

Fig. 5.1: A rapid prototyping method based on RTW.

Table 5.1: Guidance simulation with slight initial deviation and small step length.

Filtering method	Standard UKF	SSUKF	EKF
Position error /m	253.729	253.531	271.229
Velocity error /(m · s-1)	0.267	0.267	0.281
Convergence time /s	2466	2464	2469
Relative computation time	1.042	0.719	0.25

Suppose $\Delta X_0 = [2\ -2\ 2\ -2\ 2\ -2]$ the state variable has an initial deviation of a. The positioning error is defined in km. The error of the speed is expressed as m · s-1. The simulation takes 15 seconds [24]. The simulation time is four tracks. The simulation results are shown in Table 5.1 and in Figures 5.2 and 5.3. The deviation from the positioning to the rate is defined as the modulus of the deviation vector. The convergence time is the interval between the starting point and the critical point at which the estimated accuracy reaches 1 km. The results show that the SSUKF and UKF algorithms have good filter design consistency. The calculation speed of the algorithm is greatly improved. The EKF method is also the most effective and accurate in the solution process.

6. Conclusion. The work and operation process of OSS in orbit is comprehensively analyzed. The structure and working mode of the navigation system is given by selecting the OSS positioning sensor. A novel Kalman filter is constructed by combining the UKF method with the SSUT method, and it is used in the automatic astronomical navigation of spacecraft. The OSS navigation simulation experiment is carried out by using MATLAB/RTW software. The composition and implementation environment of the system, as well as some critical technologies involved, are also introduced in detail. The digital simulation of the SSUKF algorithm proves that the algorithm has the same filtering effect as the ordinary UKF algorithm. The calculation speed of the algorithm is greatly improved. A novel Kalman filter is obtained by combining the advantages of the two methods. The algorithm has good estimation accuracy, convergence speed and robustness, and higher operational efficiency. This method is suitable for autonomous positioning of spacecraft.

REFERENCES

[1] Cui, D. (2022). Application of CREAM algorithm in navigation. Academic Journal of Science and Technology, 1(2), 52-55.
[2] Shizhuang, W. A. N. G., Xingqun, Z. H. A. N., Yawei, Z. H. A. I., Cheng, C. H. I., & Jiawen, S. H. E. N. (2021). Highly

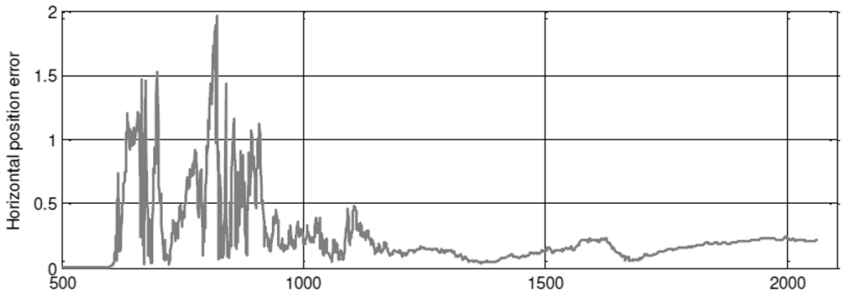

Fig. 5.2: Error estimation of positioning using SSUKF method.

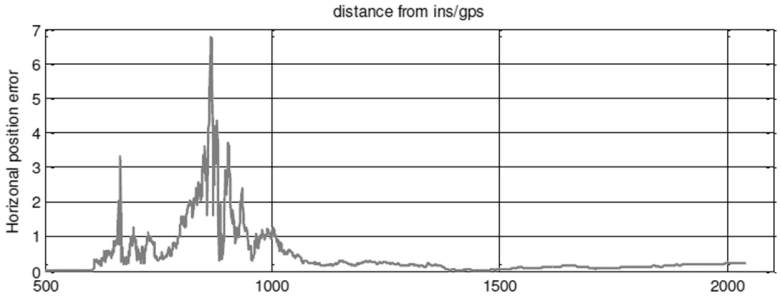

Fig. 5.3: Error analysis of speed estimation using SSUKF method.

reliable relative navigation for multi-UAV formation flight in urban environments. Chinese Journal of Aeronautics, 34(7), 257-270.

[3] Faghihinia, A., Atashgah, M. A., & Dehghan, S. M. (2021). Analytical expression for uncertainty propagation of aerial cooperative navigation. Aviation, 25(1), 10-21.

[4] Valasek, J., Harris, J., Pruchnicki, S., McCrink, M., Gregory, J., & Sizoo, D. G. (2020). Derived angle of attack and sideslip angle characterization for general aviation. Journal of Guidance, Control, and Dynamics, 43(6), 1039-1055.

[5] Chandrasekaran, K., Theningaledathil, V., & Hebbar, A. (2021). Ground based variable stability flight simulator. Aviation, 25(1), 22-34.

[6] Krasuski, K., Ćwiklak, J., Bakuła, M., & Mrozik, M. (2022). Analysis of the Determination of the Accuracy Parameter for Dual Receivers Based on EGNOS Solution in Aerial Navigation. acta mechanica et automatica, 16(4), 365-372.

[7] Erkec, T. Y., & HACIZADE, C. (2020). Relative navigation in UAV applications. International Journal of Aviation Science and Technology, 1(02), 52-65.

[8] Chernomorsky, A. I., Lelkov, K. S., & Kuris, E. D. (2020). About One way to increase the accuracy of navigation system for ground wheeled robot used in aircraft parking. Smart Science, 8(4), 219-226.

[9] Tang, Y., Zhu, F., & Chen, Y. (2021). For more reliable aviation navigation: Improving the existing assessment of airport electromagnetic environment. IEEE Instrumentation & Measurement Magazine, 24(4), 104-112.

[10] Zhang, L., Hsu, L. T., & Zhang, T. (2022). A novel INS/USBL integrated navigation scheme via factor graph optimization. IEEE Transactions on Vehicular Technology, 71(9), 9239-9249.

[11] Luo, W., Zhang, X., & Liu, X. (2020). Simulation of multi-path suppression algorithm for civil aviation satellite navigation jamming signal. Computer Simulation, 37(03), 52-56.

[12] Sun, Y., Geng, N., Gong, S., & Yang, Y. (2020). Research on improved genetic algorithm in path optimization of aviation logistics distribution center. Journal of Intelligent & Fuzzy Systems, 38(1), 29-37.

[13] Won, D., Oh, J., Kang, W., Eom, S., Lee, D., Kim, D., & Han, S. (2022). Flight Scenario Trajectory Design of Fixed Wing and Rotary Wing UAV for Integrated Navigation Performance Analysis. Journal of the Korean Society for Aviation and Aeronautics, 30(1), 38-43.

[14] Wang, S. Z., Zhan, X. Q., Zhai, Y. W., Chi, C., & Liu, X. Y. (2020). Ensuring high navigation integrity for urban air mobility using tightly coupled GNSS/INS system. J. Aeronaut. Astronaut. Aviat, 52(4), 429-442.

[15] Erkeç, T. Y., & Hajiyev, C. (2020). The methods of relative navigation of satellites formation flight. International Journal of Sustainable Aviation, 6(4), 260-279.

[16] Alnuaimi, M., & Perhinschi, M. G. (2021). Investigation of alternative parameters for immunity-based UAV navigation in GNSS-denied environment. Unmanned Systems, 9(01), 65-72.

[17] Jheng, S. L., Jan, S. S., Chen, Y. H., & Lo, S. (2020). 1090 MHz ADS-B-based wide area multilateration system for alternative positioning navigation and timing. IEEE sensors journal, 20(16), 9490-9501.
[18] Gao, D., Hu, B., Qin, F., Chang, L., & Lyu, X. (2021). A real-time gravity compensation method for INS based on BPNN. IEEE Sensors Journal, 21(12), 13584-13593.
[19] Carroll, J. D., & Canciani, A. J. (2021). Terrain-referenced navigation using a steerable-laser measurement sensor. Navigation, 68(1), 115-134.
[20] Maamo, M. S., Afonin, A. A., & Sulakov, A. S. (2022). Aircraft wing vibration parameters measurement system using MEMS IMUs and closed-loop optimal correction. Aerospace Systems, 5(3), 473-480.
[21] Zhang, L., Shaoping, W. A. N. G., Selezneva, M. S., & Neusypin, K. A. (2022). A new adaptive Kalman filter for navigation systems of carrier-based aircraft. Chinese Journal of aeronautics, 35(1), 416-425.
[22] Gabela, J., Kealy, A., Hedley, M., & Moran, B. (2021). Case study of Bayesian RAIM algorithm integrated with Spatial Feature Constraint and Fault Detection and Exclusion algorithms for multi-sensor positioning. Navigation, 68(2), 333-351.
[23] Neogi, N. A. (2020). Progress in autonomy: space robotics, satellite systems, air traffic control. Aerospace America, 58(11), 44-44.
[24] Hassan, T., El-Mowafy, A., & Wang, K. (2021). A review of system integration and current integrity monitoring methods for positioning in intelligent transport systems. IET Intelligent Transport Systems, 15(1), 43-60.

Edited by: Zhigao Zheng
*Special issue on:*Graph Powered Big Aerospace Data Processing
Received: Oct 3, 2023
Accepted: Oct 19, 2023